Experimental Study of a Cooling Coil and the Validation of its Simulation Model for the Purpose of Commissioning

Hiromasa Yamaguchi
The Kansai Electric Power Co., Inc.
Osaka, Japan

Masato Miyata
Kyoto University
Kyoto, Japan

Hisato Oda
Sinko Kogyo Co., Ltd
Osaka, Japan

Masaki Shioya
Kajima Corporation
Tokyo, Japan

Takeshi Watanabe
NTT Facilities, Inc.
Tokyo, Japan

Hideharu Niwa
Nikken Sekkei Co. Ltd
Osaka, Japan

Harunori Yoshida
Kyoto University
Kyoto, Japan

Abstract: For HVAC system commissioning, it is important to evaluate the performance of the cooling coil in an air-handling unit. However, manual evaluation requires a great deal of time and effort. One solution is to predict the coil performance by simulation. However, it remains unclear whether the currently available simulation models can provide accurate results under various operational conditions. In the present study, a slit fin type coil was investigated by conducting two series of experiments, for the VAV system and the CAV system, respectively. In addition, the accuracy of seven simulation models was examined using the experimental data.

1.INTRODUCTION

For HVAC system commissioning, it is important to evaluate the performance of the cooling coil in an Air-Handling Unit (AHU). However, manual evaluation requires a great deal of time and effort. One solution is to predict the coil performance by simulation. However, it remains unclear whether the currently available simulation models can provide accurate results under various operational conditions. In order to verify the appropriateness of using the estimation value obtained by the simulation for commissioning, it is important to validate the accuracy of the model under various operational conditions. In the present study, a slit fin type coil, which is used in most AHUs, was investigated by conducting two series of experiments, for the Variable Air Volume (VAV) system and Constant Air Volume (CAV) system, respectively. In the VAV system experiments, the exchanged heat and outlet water temperatures were measured under the conditions of changing the set point of the outlet air temperature and the air flow rate. In the CAV system experiments, the exchanged heat and outlet water temperatures were measured under a constant air flow rate and gradual variation of the water flow rate. In addition, the accuracy of seven simulation models was examined using the experimental data.

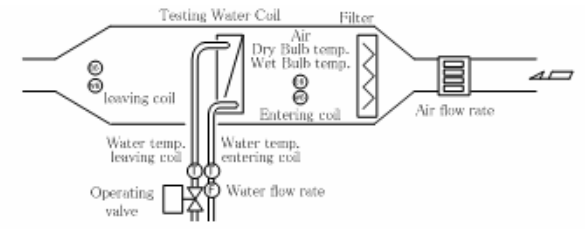

Fig. 1Schematic diagram of the experimental

2. EXPERIMENT

2.1 Outline of the Experiment

In the present study, two series of experiments were conducted to examine the Variable Air Volume (VAV) system and the Constant Air Volume (CAV) system, respectively. In these experiments, the air/water outlet value was measured under the stable condition of maintaining constant the air/water inlet value. The specifications of the coil used in the experiment are shown in Table 1, and a schematic diagram of the experimental apparatus is shown in Figure 1.

Tab. 1 The specification of coil for the experime

Specification	Number of rows of the tubes		6
	Number of tubes per rows		12
	Flow type		Quarter flow
	Size	height	456mm
		width	500mm
	Tube	material	Copper
		outside diameter	16.1 mm
		inside diameter	15.1 mm
	Fin	material	Slit fin aluminum
		spacing	3.3mm
		thickness	0.15mm
Design conditions	Air flow rate (velocity)		2100 m³/h(2.6 m/s)
	Cooling performance		16.6 kW
	Inlet air temp.		28°CDB / 22°CWB
	Outlet air temp.		15°CDB / 14.5°CWB
	Inlet/Outlet water temp.		7°C / 14°C
	Water flow rate (velocity)		34 L/min(1.05 m/s)

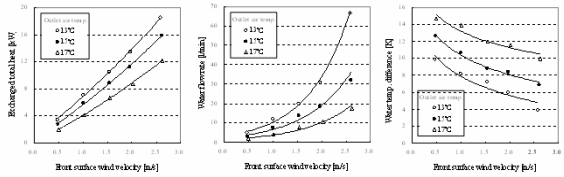

Fig. 2 Experimental results for the VAV system

Tab. 2 Conditions of the VAV system experiments

(Inlet Conditions)
Air temp. 28 °C DB／22 °C WB
Water temp. 7 °C

Front surface wind velocity	Set point of outlet air temp.		
	13 °C	15 °C	17 °C
0.5 m/s（20%）	Exp1	Exp6	Exp11
1.0 m/s（40%）	Exp2	Exp7	Exp12
1.6 m/s（60%）	Exp3	Exp8	Exp13
2.1 m/s（80%）	Exp4	Exp9	Exp14
2.6 m/s（100%）	Exp5	Exp10	Exp15

Tab.3 Conditions of the CAV system

Inlet Conditions)
Air temp. 28 °C DB／22 °C WB
Front surface wind velocity 2.6 m/s
Water temp. 5 °C,7 °C,10 °C,15 °C,20 °C

Water velocity [m/s] （Water flow rate [l/min]）							
0.05 (1.6)	0.1 (3.2)	0.25 (8.1)	0.5 (16)	0.75 (24)	1.0 (34)	1.5 (49)	2.0 (65)

2.1.1VAV system Experiment

In the VAV system experiments, the outlet air temperature/humidity, the outlet water temperature, and the water flow rate were measured under constant outlet air temperature by two-way valve control and by varying the set point and air flow rate. The air flow rate was fixed for five stages between 0.5 ~ 2.6 m/s as for the front surface wind velocity. The set points of the outlet air temperatures for three stages were 13, 15, and 17°C. The inlet air temperature was maintained at 28°C DB/22°C WB, and the inlet water temperature was maintained as 7°C. The conditions of the VAV system experiment are shown in Table 2.

2.1.2CAV system Experiment

In the CAV system experiments, the outlet air temperature/humidity and the outlet water temperature were measured while maintaining the air flow rate constant and varying the water flow rate gradually. The water flow rate was adjusted in an attempt to achieve the value shown in Table 3. However, the actual water flow rate does not agree exactly with the value shown in Table 3, because the two-way valve was adjusted manually. A number of experiments were performed at smaller intervals than those listed in the Table. The inlet air temperature was maintained at 28°C DB/22°C WB, and the inlet water temperature was set for the following five stages: 5, 7, 10, 15, and 20°C.

2.2 Experimental result

2.2.1Experimental result for the VAV system

The experimental results for the VAV system (exchanged total heat, water flow rate, and difference between inlet and outlet water temperatures) are shown in Figure 2. For all of the three set points of the outlet air temperature, the cooling performance has a tendency to be increased in proportion to the air flow rate. For the case in which the outlet air temperature is set to 13°C, the cooling performance exceeds the design value (16.6 kW) by approximately 11%. On the other hand, the required water flow rate becomes approximately twice the design value (34 L/min). It is difficult to perform such operations in an actual HVAC system, because there is a limit in the flow rate of the pump. When the air flow rate decreases, the water temperature difference tends to increase because the proportion of the heat exchange area to the heating exchange quantity increases. This indicates that the phenomenon whereby the water temperature difference decreases for a low cooling load is not caused the coil performance, but rather is caused by the plumbing and the control system.

2.2.2 Experimental results for the CAV system

The experimental results for the CAV system (exchanged latent heat, difference between inlet and outlet water temperature, and outlet air temperature) are shown in Figure 3. Overall, the cooling

performance has a tendency to increase in proportion to the water flow rate. Even beyond the design water flow rate, this tendency holds. However, the limit (4 kW) is reached when the outlet water temperature is 20°C, and latent heat exchange occurs only slightly. When the water flow rate decreases, the water temperature difference tends to increase. The maximum difference is 20 K for the case in which the outlet water temperature is 5°C. The outlet air temperature tends to decrease with the increase in the water flow rate. The sensible heat ratio also decreases with the increase in the water flow rate. The difference between the inlet water temperature and the outlet air temperature (8 K in design) is 2 K in the case of the outlet water temperature 5°C.

3. ALGORITHM OF THE COIL MODEL

The following seven simulation models of the cooling coil were selected for comparison with the experiment results. The detailed description is omitted herein, and only the main characteristic is shown. For the details of the algorithm of each model, please refer to the references. Furthermore, all of the models are static, except for HVACSIM+Type602. The static model was selected for use in the present study, although SIMBAD provides both static and dynamic models. TRNSYS Type52 can be applied to dynamic simulation, by incorporating a subroutine.

1) HASP/ACSS/8502 cooling/warming coil [1)]
2) HVACSIM+ Type602 [2,3)]
3) SIMBAD Detailed static cooling coil [4)]
4) ASHRAE Type63 [5)]
5) Niitsu model [6)]
6) TRNSYS Type52 [7)]
7) Calculation method using the coefficient of the wet surface[8)]

* In the following sentences, names of the model are abbreviated as follows. “ACSS, HVACSIM+, SIMBAD, ASHRAE, NIITSU, TRNSYS, and wet surface”.

3.1. HASP/ACSS/8502 cooling/warming coil

This model calculates the outlet water temperature and water flow rate, based on the input inlet/outlet air temperature/humidity, the inlet water temperature and air flow rate, and the outlet water temperature and water flow rate. This model distinguishes the coil for the dry regime and the wet regime at the boundary point, which is 95% of the relative humidity. By solving the simultaneous equations of equation (1) and the heat balance equations of the air side and water side, the solution is obtained. The original model replaces equations (2) and (3) with a simple equivalence coil that does not distinguish between the dry and wet regimes in order to simplify calculation. However, in the present study, equations (2) and (3) are used directly. The overall heat exchange coefficient is approximated by equations (4) and (5).

$$A_0 = A_{dry} + A_{wet} \tag{1}$$

$$A_{dry} = Q_{dry} / (k_{dry} \cdot mtd) \tag{2}$$

$$A_{wet} = Q_{wet} / (k_{wet} \cdot mhd) \tag{3}$$

$$U_{dry} = \left\{ a_1 v_w^{(-0.8)} + b_1 + c_1 v_a^{(-0.64)} \right\}^{-1} \tag{4}$$

$$U_{wet} = \left\{ a_2 v_w^{(-0.8)} + b_2 + c_2 v_a^{(-0.8)} \right\}^{-1} \tag{5}$$

Here,

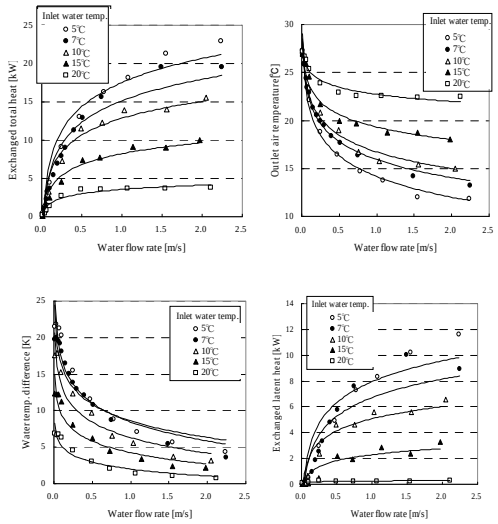

Fig. 3 Experimental results for the CAV

$$mtd = \frac{\left((\theta_{ai} - \theta_{wo}) - (\theta_{a,bd} - \theta_{w,bd})\right)}{\ln \dfrac{\theta_{ai} - \theta_{wo}}{\theta_{a,bd} - \theta_{w,bd}}}$$

$$mhd = \left((h_{a,bd} - h_{w,bd}) - (h_{ao} - h_{wi})\right) \Big/ \ln \frac{h_{a,bd} - h_{w,bd}}{h_{ao} - h_{wi}}$$

$a_1 = 0.00569,\quad b_1 = 0.00547,\quad c_1 = 0.0310$

$a_2 = 0.00290,\quad b_2 = 0.00279,\quad c_2 = 0.0110$

A_0 : coil surface area [m^2], A_{dry} : surface area for the dry regime [m^2], A_{wet} : surface area for the wet regime [m^2], Q_{dry} : exchanged heat for the dry regime [kW],

Q_{wet} : exchanged heat for the wet regime [kW], U_{dry} : overall heat exchange coefficient for the dry regime [kW/(m^{2}K)], U_{wet} : overall heat exchange coefficient for the dry regime [kW/(m^{2}K)], mtd : logarithm average difference in temperature for the dry regime [°C], mhd : logarithm average enthalpy difference for the wet regime [kJ/kgDA], v_w : water velocity in the pipe [m/s], v_a : front surface wind velocity [m/s], θ_{ai} : inlet dry bulb air temperature [°C], $\theta_{a,bd}$: dry bulb air temperature at the dry/wet boundary [°C], θ_{wo} : outlet water temperature [°C], $\theta_{w,bd}$: water temperature at the dry/wet boundary [°C], $h_{a,bd}$: enthalpy of air at the dry/wet boundary [kJ/(kgDA)], $h_{w,bd}$: enthalpy of saturated air with respect to water temperature $\theta_{w,bd}$ [kJ/(kgDA)], h_{ao} : enthalpy of outlet air [kJ/(kgDA)], and h_{wi} : enthalpy of saturated air with respect to water temperature θ_{wi} [kJ/(kgDA)].

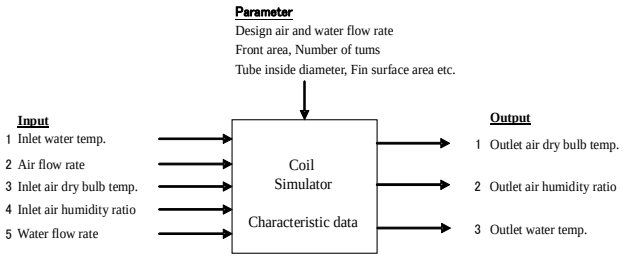

Fig.4 put and output for the simulation

3.2. HVACSIM+ Type602

This model selects one from the following three cases by the condition of the surface of the coil, all dry coil, all wet coil, and partially wet coil. This model calculates the outlet conditions of air and water, the exchanged heat, the input inlet conditions of air and water, the air flow rate, and the water flow rate by solving the simultaneous equations of equations (6) and (7) and the heat balance equations for air and water. The overall heat exchange coefficient is calculated using equations (8) and (9). In the case of the partially wet coil, the coil surface is classified into dry regime and wet regime regions, and the boundary is calculated by repeated calculations. Furthermore, each output is calculated by adding a dynamic element using equations (10) - (12).

$$Q_{dry} = U \cdot A_0 \cdot mtd \tag{6}$$

$$Q_{wet} = U_c \cdot A_0 \cdot mhd \tag{7}$$

$$\frac{1}{UA_0} = \frac{1}{f_0 A_0 \eta_0} + \frac{F_t}{K_t A_i} + \frac{1}{f_i A_i} + \frac{F}{A_i} \tag{8}$$

$$\frac{1}{U_c A_0} = b\left(\frac{1}{b f_{0w} A_0 \eta_{0w}} + \frac{F_t}{K_t A_i} + \frac{1}{f_i A_i} + \frac{F}{A_i} \right) \tag{9}$$

$$\frac{C_m}{UA_0} \cdot \frac{d\theta'_{ao}}{dt} = \theta_{ao} - \theta'_{ao} \tag{10}$$

$$\frac{C_m}{UA_0} \cdot \frac{d\theta'_{wo}}{dt} = \theta_{wo} - \theta'_{wo} \tag{11}$$

$$\frac{C_m}{UA_0} \cdot \frac{dx'_{ao}}{dt} = x_{ao} - x'_{ao} \tag{12}$$

U : overall heat exchange coefficient based on mtd [kW/(m^{2}K)], U_c : overall heat exchange coefficient based on mhd [kW/(m^{2}K)], f_0 : air side transfer coefficient for the dry regime [kW/(m^{2}K)], η_0 : efficiency of the fins for the dry regime [-], F_t : fin thickness [m], K_t : tube conductivity [kW/(mK)], A_i : inside surface area of the tube [m^2], f_i : water side transfer coefficient [kW/(m^{2}K)], F : coil fouling factor [(m^{2}K)/kW], f_{0w} : air side transfer coefficient for the wet regime [kW/(m^2･K)], η_{0w} : efficiency of the fins for the wet regime [-], C_m : coil heat capacity [kJ/K], and x_{ao} : outlet air humidity ratio [kg/kgDA].

3.3 SIMBAD detailed static cooling coil

The basic algorithm is similar to ASHRAE Type63, but the parameters and the approximation equation to calculate R_a, R_m, and R_w are different. In addition, three kinds of cooling coil models of the simple static cooling coil, the simple dynamic cooling coil, and the detailed dynamic cooling coil are available for SIMBAD.

3.4. ASHRAE Type63

This model selects one from the following three cases by the condition of the surface of the coil, all dry coil, all wet coil, and partially wet coil. This model calculates the exchanged total heat Q_t and the bypass factor B_f based on the input inlet conditions of air and water, air flow rate, and water flow rate from equations (13) and (14). Using Q_t and B_f and the heat balance equations for air and water, the outlet conditions for air and water are

calculated. The characteristics of this model are that the entire surface is treated as an average condition, without classifying the coil surface into the dry regime and the wet regime.

$$Q_t = \varepsilon \cdot C_{\min}(\theta_{ai} - \theta_{wi}) \quad (13)$$

$$B_f = \exp\left(\frac{-A_0}{C_{air} \cdot R_a}\right) \quad (14)$$

$$\varepsilon_c = f(U_c, C_{air}, C_{water}) \quad (15)$$

$$UA = \frac{A_0}{R_a + R_m + R_w} \quad (16)$$

$$C_{\min} = \min(C_{air}, C_{water}) \quad (17)$$

$$C_{air} = \dot{m}_a(c_{pa} + c_{px}x_{ai}) \quad (18)$$

$$C_{water} = \dot{m}_w c_{pw} \quad (19)$$

ε_c : efficiency of exchanger [-], x_{ai} : inlet air humidity ratio [kg/kgDA], θ_{wi} : inlet water temperature [°C], $\dot{m}_a$: air flow rate [kg/s], $\dot{m}_w$: water flow rate [kg/s], c_{pa} : constant pressure specific heat of air [J/kgK], c_{px} : constant pressure specific heat of vapor [J/kgK], c_{pw} : specific heat of water [J/kgK], R_a : air side thermal resistance [m^2K/kW], R_m : resistance of the metal [m^2K/kW], and R_w : water side thermal resistance [m^2K /kW].

3.5. Niitsu model

The imaginary fin surface is set up for each row of the coil. This model assumes that heat transfer and mass transfer are achieved through the imaginary fin surface. The heat balance of the entire coil is expressed by equation (20). The heat balance in the imaginary fin surface of the n[th] row is expressed by equations (21) - (23).

$$Q_{ct} = \sum_{n=1}^{N}\left(q_{s,n} + q_{l,n}\right) = \sum_{n=1}^{N} q_{w,n} \quad (20)$$

$$q_{s,n} = \alpha_{a,n} A_a \left(\frac{\theta_{ca,n} + \theta_{ca,(n+1)}}{2} - \theta_{f,n}\right) \quad (21)$$

$$q_{l,n} = k_{x,n} A_a \left(\frac{x_{ca,n} + x_{ca,(n+1)}}{2} - x_{f,n}\right) r_n \quad (22)$$

$$q_{w,n} = \alpha_{w,n} A_w \left(\theta_{f,n} - \frac{\theta_{cw,n} + \theta_{cw,(n+1)}}{2}\right) \quad (23)$$

$q_{s,n}$: sensible heat transfer in the n[th] row [kW], $q_{l,n}$: latent heat transfer in the n[th] row [kW], $q_{w,n}$: water side heat transfer in the n[th] row [kW], N : number of rows [-], $\alpha_{a,n}$: air side transfer coefficient in the n[th] imaginary fin surface [W/m^2K], A_a : air side surface area in a row [m^2], $\theta_{ca,n}$: inlet air temperature in the n[th] row [°C], $\theta_{f,n}$: temperature of the imaginary fin surface in the n[th] row [°C], $k_{x,n}$: air side substance transmission rate based on absolute humidity in the n[th] row [1/(m^2skgDA)], $x_{ca,n}$: inlet air humidity ratio in the n[th] row [kg/kgDA], $x_{f,n}$: humidity ratio of the saturated air equivalent to the imaginary fin surface temperature [kg/kgDA], r_n : latent heat of vaporization in the n[th] row [kJ/kg], $\alpha_{w,n}$: water side transfer coefficient in the n[th] imaginary fin surface [W/m^2·K], A_w : water side surface area in a row [m^2], and $\theta_{cw,n}$: inlet water temperature in the n[th] row [°C].

3.6. TRNSYS Type52

This model selects one from the following three cases by the condition of the surface of the coil, all dry coil, all wet coil, and partially wet coil. Inputs and outputs are similar to those of HVACSIM+. In this model the number of heat transfer units inside (NTUI) and the number of heat transfer units outside (NTUO) are calculated using f_0, f_i, and η_0, for example. Combining these values, the number of heat transfer units for the case in which the outside surface is dry (NTUD) and that for the case in which the outside surface is wet (NTUW) are calculated. Furthermore, the outlet water/air condition is calculated using the coil efficiency (EPS), which is calculated from NTUD and NTUW. For the case of the partially wet coil, the coil surface is classified as dry regime and wet regime, and the dry surface ratio (KDRY) is calculated by repeated calculations. The

calculation method used to determine the outlet conditions in the case of the dry coil is shown in equations (24) and (25).

$$\theta_{w,bd} = \theta_{wi} + EPSD \cdot CSTAR \cdot (\theta_{ai} - \theta_{wi}) \quad (24)$$

$$\theta_{a,bd} = \theta_{ai} - EPSD \cdot (\theta_{ai} - \theta_{wi}) \quad (25)$$

Here,

$(TEMP < 50)$

$EPSD = (1 - EXP(TEMP)) / (1 - CSTAR \cdot EXP(TEMP))$

$(TEMP \geq 50) \quad EPSD = 1/CSTAR$

$TEMP = -NTUD \cdot (1 - CSTAR)$

$CSTAR = \dot{m}_a \cdot c_{pa} / (\dot{m}_w \cdot c_{pw})$

$NTUD = NTUO / (1 + NTUO / NTUI \cdot CSTAR)$

$NTUI = A_i / \{(1/f_i + 1/K_t) \cdot (\dot{m}_w \cdot c_{pw})\}$

$NTUO = \eta_0 \cdot f_0 \cdot AO / (\dot{m}_a \cdot c_{pm})$

AO : outside surface area of tube [m^2], and c_{pm} : wet air specific heat [kJ/(kg·K)].

3.7. Calculation method using the coefficient of the wet surface

This model calculates the coil performance using the coefficient of the wet surface, which is used in the design of the number of rows. By solving the simultaneous equations of equation (26) and the heat balance equations for air and water, the solution is obtained. Commonly, the approximation equations for the heat transfer coefficient K_f and the wet surface coefficient WSF are obtained from the AHU maker. The relative humidity of the outlet air is assumed to be 95%.

$$Q_t = WSF \cdot K_f \cdot A_{ext} \cdot N \cdot MTD \quad (26)$$

Here,

$K_f = 37.912 / (0.059416 \cdot v_a^{-0.47321} + 0.0082317 \cdot v_w^{-0.78318})$

$WSF = 1.04 \cdot SHF^2 - 2.63 \cdot SHF + 2.59$

MTD : logarithm average difference in temperature [^{o}C]

4. RESULTS OF THE SIMULATION

The reappearance simulation of the experiment was implemented using seven cooling coil models. The input-output differs by model. By changing the algorithm, the input-output was unified as shown in Figure 4.

4.1. Simulation results for the VAV system

Tab. 4 RMSE of the experiment and calculation of the VAV

	SIMBAD	ASHRAE	NIITSU	ACSS	HVAC SIM+	TRNSYS	Wet surface
Outlet air temp.[°C]	1.4	3.6	2.3	1.0	1.0	2.2	0.4
Outlet air humidity ratio[kg/kg']	0.0006	0.0011	0.0002	0.0004	0.0003	0.0018	0.0005
Outlet water temp.[°C]	1.1	1.9	0.7	0.5	0.3	2.6	1.2
Exchanged sensible heat [kW]	0.5	1.8	0.9	0.5	0.3	1.2	0.2
Exchanged total heat[kW]	0.8	2.7	0.9	1.1	0.2	3.7	0.4
SHF[-]	0.03	0.12	0.04	0.01	0.04	0.15	0.02

The experimental value of the simulation was input. The input-output of the simulation of the VAV system is shown in Figures 5 and 6. The root mean square error (RMSE) of the experimental values and the calculation values are shown in Table 4 for all cases. The horizontal axes of Figures 5 and 6 show the experimental cases of Table 2.

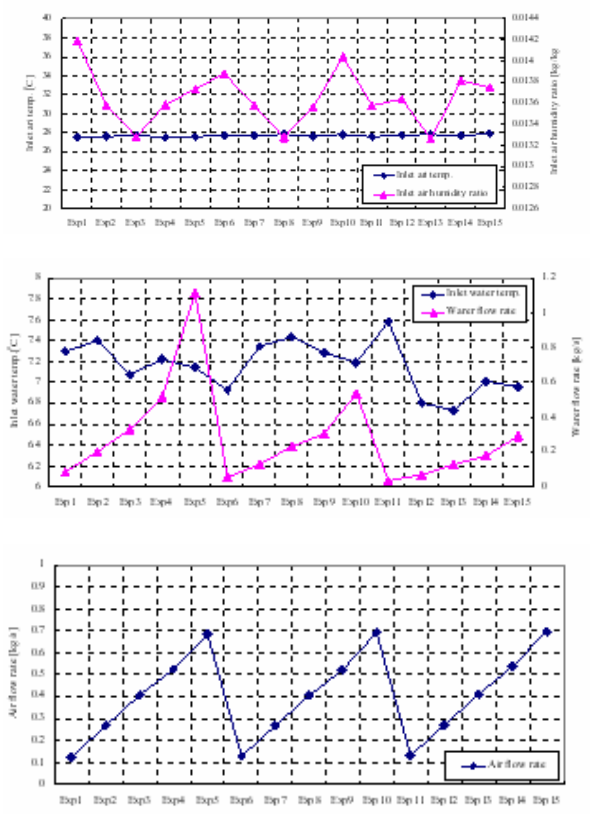

Fig.5 Simulation input for the VAV

The outlet air dry bulb temperature has a tendency to be calculated slightly higher than the experimental result. The results for the wet surface are the most accurate. For the case in which the setting value of the outlet air temperature is 13 or 15°C, HVACSIM+ calculated the next closest result to the experimental results. In the case of the 17^{o}C setting, ACSS was the next closest. Niitsu has the highest accuracy for the outlet air humidity ratio, followed by HVACSIM+. ACSS has a tendency to be calculated as accurately as the dry bulb temperature in the case of the 17°C setting. HVACSIM+ has the highest accuracy for the outlet water temperature, followed by ACSS. On the

whole, the calculated value is slightly lower than the experimental value. The calculation accuracy of the exchanged heat is highest for HVACSIM+, followed by SIMBAD and ACSS, in order. On the whole, the calculated value is slightly less than the experimental value. The calculation errors for the sensible heat ratio (SHF) were not preferentially distributed in one direction.4.2 Simulation results for the CAV system

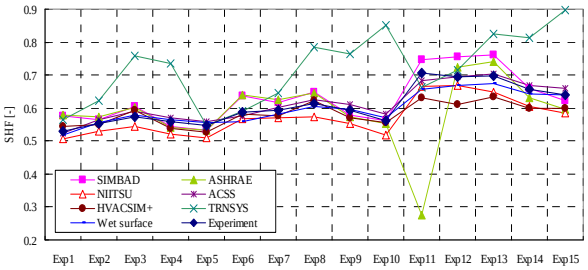

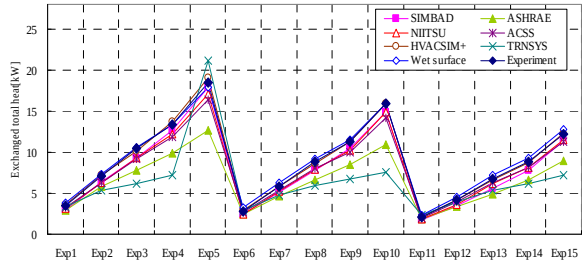

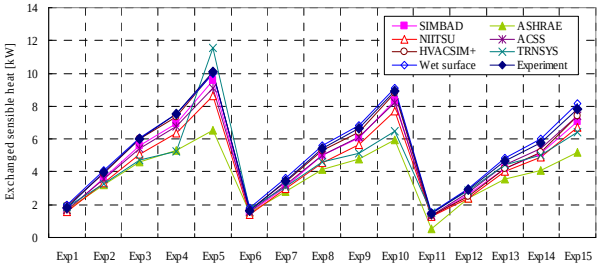

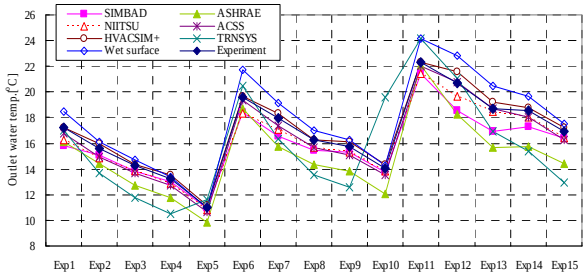

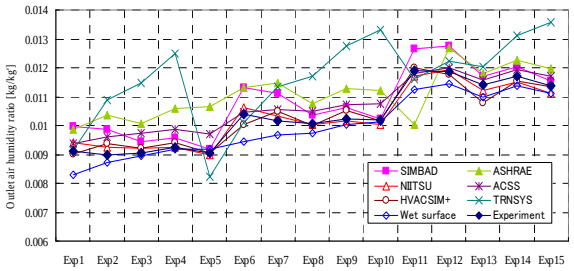

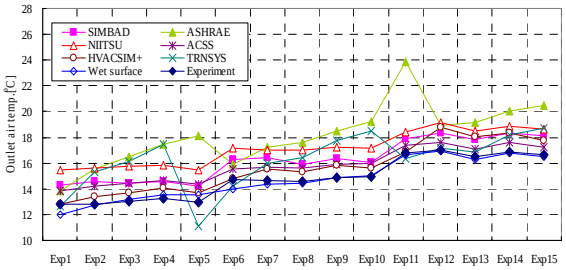

Fig.6 Simulation output for the VAV system

The input-output of the simulation of the CAV system is shown in Figures 7 and 8. The RMSE of the experiment values and the calculation values for all cases are shown to Table 5. The horizontal axes of Figures 7 and 8 indicate the experiment case. The inlet water temperature in equations 34 ~ 43 is 5°C, that in equations 1 ~ 14 is 7°C, that in equations 15 ~ 23 is 10°C, that in equations 24 ~ 33 is 15°C, and that in equations 44 ~ 53 is 20°C. For the case of the same inlet water temperature, the larger the number, the higher the water flow rate.

As with the VAV system, the CAV system has a tendency for the exchanged heat to be calculated slightly lower and the outlet air dry bulb temperature to be calculated slightly higher. With respect to the outlet air temperature, the wet surface was the most accurate, followed by SIMBAD and ACSS, which showed high accuracy in the case of a low water flow rate, and HVACSIM+ shows a high accuracy in the case of a high water flow rate. The wet surface, Niitsu, and SIMBAD had high accuracy over a wide range with respect to the outlet air humidity ratio. However, for Niitsu, the emission in the case of a low water flow rate was observed. The calculation accuracy of the exchanged heat was highest for the wet surface, followed by HVACSIM+ and SIMBAD, in order. However, the error of SIMBAD increased for the exchanged sensible heat in the case of the inlet water temperature of 20°C. For the sensible heat ratio (SHF), HVACSIM+ showed a large error. TRNSYS showed a different tendency compared to the other models for both the VAV and CAV systems. TRNSYS Type52 was able to adapt only the single flow coil. In the present study, the parameters such as the number of tubes per rows, etc. were changed to more closely approach the water velocity in the pipe given by the specifications of the experimental coil. This is thought to be one of the causes that TRNSYS showed a different tendency compared to the other models. 5.

Tab. 5 RMSE of the experiment and calculation of the CAV

	SIMBAD	ASHRAE	NIITSU	ACSS	HVAC SIM+	TRNSYS	Wet surface
Outlet air temp.[°C]	0.8	1.3	1.4	0.7	1.1	1.8	0.3
Outlet air humidity ratio[kg/kg']	0.0002	0.0003	0.0002	0.0004	0.0004	0.0015	0.0002
Outlet water temp.[°C]	0.7	0.9	1.7	0.3	0.3	1.9	0.6
exchanged sensible heat[kW]	0.5	0.9	0.8	0.5	0.7	1.3	0.3
exchanged total heat[kW]	0.8	1.4	0.8	1.0	0.3	3.9	0.4
SHF[-]	0.12	0.22	0.06	0.12	0.25	0.20	0.12

various conditions were carried out for the purpose of understanding the characteristics of the cooling coil. In addition, for the purpose of validating the models, the reappearance calculations were implemented and

5. CONCLUSIONS

Experiments to examine various cases for

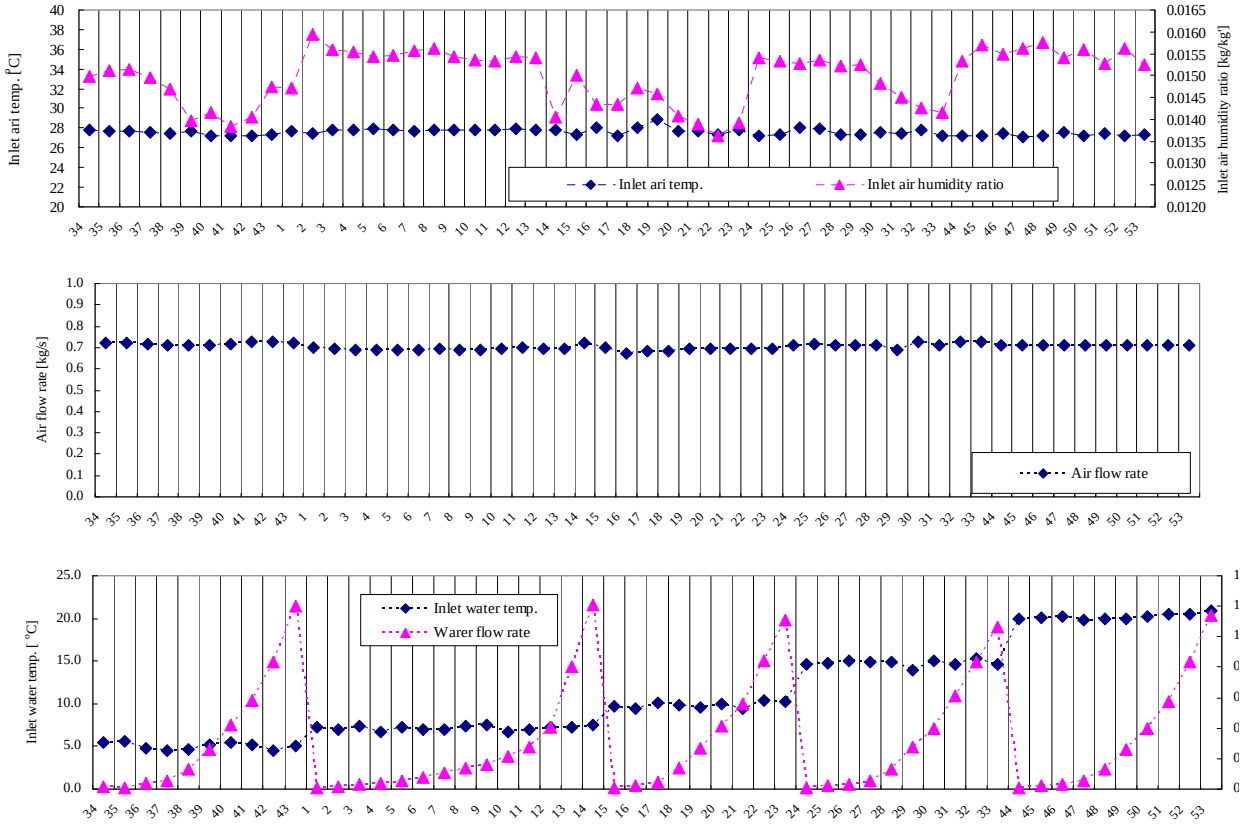

Fig. 7 Simulation input for the CAV system

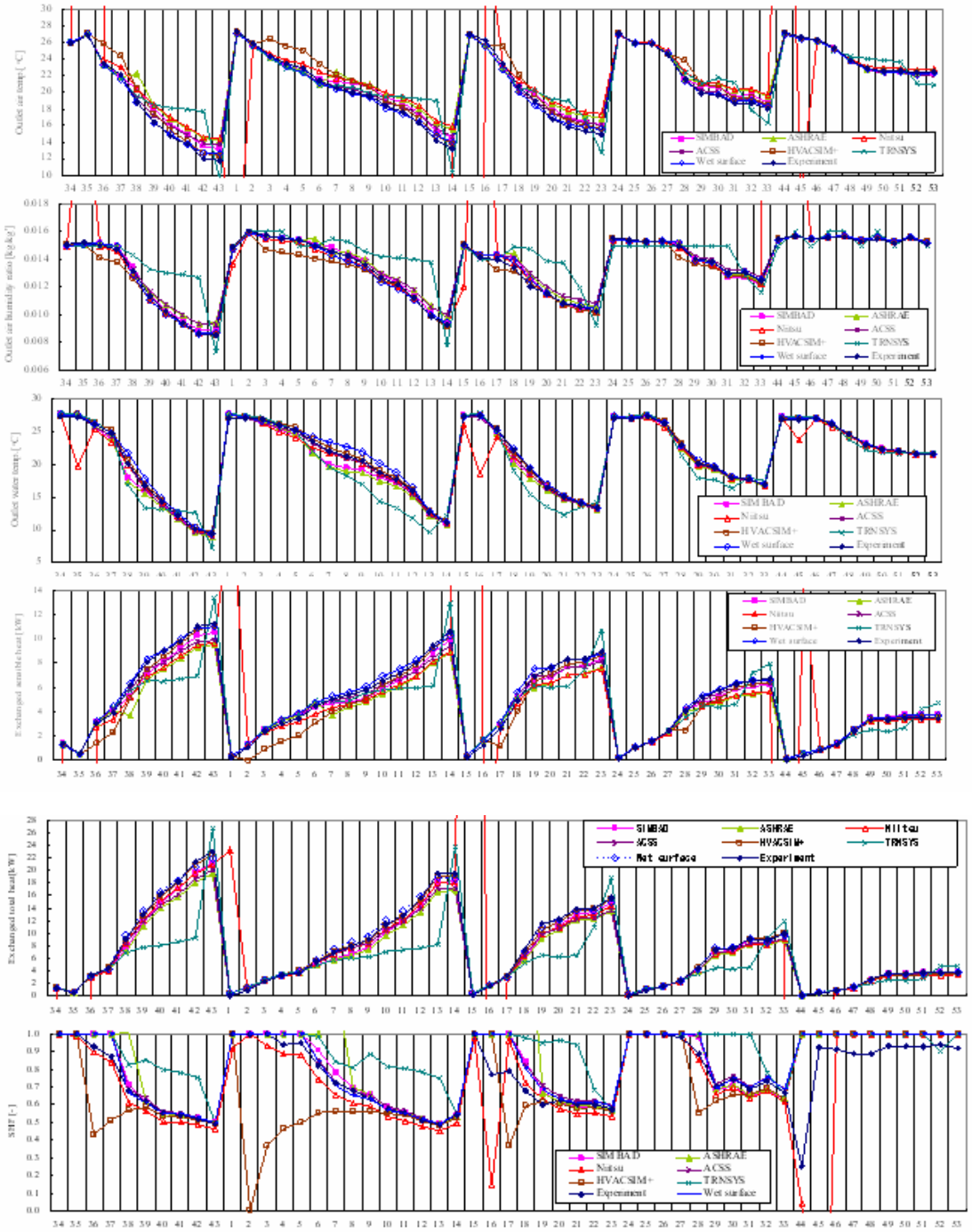

Fig 8 Simulation output for the CAV system

the results were compared with the experiment value. It is desirable to select an appropriate model according to the purpose, because the model accuracy differs with respect to the calculation item.

REFERENCES

[1] Tatsuo Inooka, Yo Matsuo, Koichi Yokoyama：HASP/ACSS：Simulation Program for Energy Consumption of Air Conditioning Systems, IBPSA International Building Energy Simulation Conference 1985, Seattle, USA

[2] A.H.Elmahdy et al；A Simple Model for Cooling and Dehumidifying Coils for Use in Calculating Energy Requirements for Buildings, ASHRAE Transactions, Paper No.2456, Vol. 83 Part 2, 1977

[3] Elmahdy,A.H. and Biggs, R.C., "Finned Tube Heat Exchanger: Correlation of Dry Surface Heat Transfer Data",ASHRAE Transactions, Vol.85, Part 2, pp.262-273, 1979

[4] Husaunndee A., Riederer P. et Visier J.C., Coil modelling in the Simbad toolbox -numerical and experimental validation of the cooling coil model, SSB'98 System Simulation in Buildings Conference,

Liège, December 14-16, 1998.

[5] Cooling Coil Models to be used in Transient and/or Wet Regimes -- Theorical Analysis and Experimental Validation.

X.DING, J-P EPPE, J.LEBRUN, M.WASACZ., I.E.A. ANNEX17 document AN17-901019-01.

[6] Yasushi Niitsu, Kazuo Naitou：Studies on Characteristics of Heat-Exchangers with Fins and its Design, Journal of SHASE Vol.39, No.4, pp.8-22，1965

[7]ASHRAE Equipment Guide, American Society of Heating, Refrigerating, and Air Conditioning Engineers, Atlanta, 1983

[8] SHASE Handbook 3 (Ver.13)，pp.248～250